IOP Conf. Series: Materials Science and Engineering **208** (2017) 012007 doi:10.1088/1757-899X/208/1/012007

Elastic properties of magnetorheological elastomer: description with the two-particle mesoscopic model

A M Biller, O V Stolbov and Yu L Raikher

Institute of Continuous Media Mechanics UB RAS, 1, Acad. Korolev St., Perm, 614013, Russia

E-mail: kam@icmm.ru

Abstract. A pair of magnetizable solid particles embedded in a cylinder made of high-elasticity material is considered as a model of a mesoscopic structure element of a magnetorheological elastomer. An applied magnetic field induces ponderomotive interaction of the particles making them to move relative to one another so as to balance the counteracting magnetic and elastic forces. In a certain parameter range, the system exhibits bistability due to which under the increase / decrease of the field, the interparticle distance changes in a hysteretic manner. This behavior has a significant effect on the ability of the mesoscopic element to resist external load. Using the developed two-particle model prone to the magnetomechanical hysteresis, we extend it to the case of a virtually macroscopic sample presenting the latter as a superposition of such elements with distributed interparticle distances. In spite of its simplicity, this scheme in a generally correct way describes the field-induced changes of the internal structure and elastic modulus of the magnetorheological composites.

1. Introduction

Magnetorheological elastomers (MREs) are a special type of smart composites distinguished by their ability for significant shape and elastic properties changes in response to applied magnetic field. Under magnetization, the microparticles of the ferromagnet filler are got coupled by ponderomotive forces that entails a number of interesting effects: magnetically induced deformation and stiffening of MREs, the magnetic shape memory, and others, all of which possessing a substantial practical potential. At the qualitative level, the picture is simple. The applied external field magnetizes the particles and imparts magnetic moments to them. The arising ponderomotive interaction strives to arrange the particles into a spatial structure that corresponds to the minimum of magnetostatic energy. For the particles embedded in a polymer, this tendency is opposed by the elastic restoring forces, which turn up in the MRE matrix as soon as any particle shifts from its initial position. Both experiment [1, 2, 3] and theory [4, 5, 6] show that such changes can strongly modify the properties of simulated MRE samples, thus entailing their qualitatively different behavior. The key issue underlying these peculiarities is the magneto-elastic interaction of the particles in a magnetorheological elastomer at the mesoscopic level, i.e., at the scale of the particle size and the interparticle distance.

2. Mesoscopic element

To clarify the above-mentioned points, in our works [7, 8] we considered a system consisting of a pair of spherical magnetizable particles embedded in an elastomer matrix. Such a mesoscopic

system is the smallest representative entity that displays basic magnetomechanical effects inherent to MREs. The scheme is illustrated in figure 1. Two particles of identical radius a are

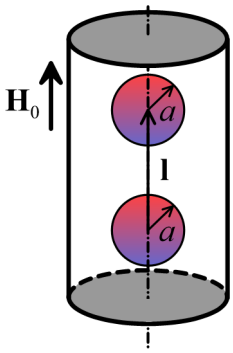

Figure 1. Schematic view of the mesoscopic element.

positioned insde an elastomer cylinder in such a way that the center-to-center line points along its axis. The outer dimensions of this two-particle (2P) element: length L_0 and cross section area S, are chosen so that the particles occupy 30% of its geometric volume; this reference value of the volume content of ferromagnetic phase is most interesting for applications.

An external magnetic field $\mathbf{H}_0$ is applied along the axis of the cylinder. Under the action of the field, the particles magnetize and get involved in the magnetostatic (ponderomotive) interaction that in the configuration of figure 1 results in mutual attraction. The magnetic energy U_{mag} of the pair depends on the center-to-center distance $l = |\mathbf{l}|$ and the magnitude of the applied field $H_0 = |\mathbf{H}_0|$ assuming minimum when the particles come into tight contact.

As full adhesion at the particle-elastomer interface is assumed, this implies that any particle displacement causes deformation of the matrix. As the polymer is non-magnetic, the elastic energy U_{el} accumulated due to that, is independent of the magnetic field being a function of only the initial l_0 and actual l distances between the particles; apparently, U_{el} is minimal in the absence of deformations ($l = l_0$).

Given that, the total energy U of the considered 2P cylindrical element of a MRE could be presented as a sum of the magnetic U_{mag} and elastic U_{el} contributions. Accordingly, under the action of external magnetic field two types of forces, competing with each other, arise inside the system: the magnetic forces tending to bring the particles closer, and the elastic ones resisting any deformation of the matrix. The algorithm that enables one to evaluate the total energy of the considered mesoscopic element, is similar to that described in our paper [8]. In below we adduce it briefly focusing on the modification made to the model and on the characteristic properties of the considered system.

The magnetic part U_{mag} of the total energy is considered, as in Ref. [8] using the numerical solution of the magnetostatic problem for two spherical particles, whose magnetization $\mathbf{M}$ is related to the internal field by the empirical Fröhlich-Kennelly formula [9], so that the magnetic response of the particles is described by two material parameters: the initial magnetic susceptibility χ_0 and the saturation magnetization M_s. For carbonyl iron particles, most commonly used as MRE fillers, the corresponding reference values are $\chi_0 \sim 10^4$ and $M_s \sim 1500$ kA/m. However, in below we use for U_{mag} dimensionless units denoting: the field intensity as $h_0 = H_0/M_s$, the distance between the particle centers as $q = l/a$ and the magnetic energy as $\tilde{U}_{mag}(q, h_0) = U_{mag}(l, H_0)/(\mu_0 M_s^2 a^3)$ with μ_0 being the magnetic permeability of vacuum.

When treating the elastic energy U_{el} induced by the particle displacements in the matrix, the approach of Ref. [8] was modified by assuming that the sample has finite dimensions. Since the elastomer can undergo significant deformations, we describe it as an incompressible Mooney-

Rivlin body [10]. The emerging nonlinear elasticity boundary problem was formulated as an axisymmetrical one and solved by the finite element method. The constants of the model, viz. c_1 and c_2, determine the elastic properties of the polymer matrix and are directly connected with its shear modulus G. To pass to dimensionless units, we introduce parameter $\tilde{c}_2 = c_2/c_1$ and elastic energy $\tilde{U}_{el}(q, q_0) = U_{el}(l, l_0)/(c_1 a^3)$. The MREs, which display the highest magnetically induced deformation and stiffening, have small Young moduli ($E \simeq 10 - 30$ kPa), see for example [11]. Taking that as a reference value, one finds that for a MRE with Young modulus $E \sim 25$ kPa the elastic constant c_1 of our model equals to 1.1 kPa for a fixed $\tilde{c}_2 = 0.2$.

To enable analytic calculations, the numerical data for the magnetic and elastic components of the energy were interpolated and their sum arranged in the functional form:

$$U(q, q_0, h_0)/(c_1 a^3) = \beta \tilde{U}_{mag}(q, h_0) + \tilde{U}_{el}(q, q_0), \tag{1}$$

which proved to be a good approximation for the true magnetoelastic energy of the mesoscopic element. As seen from (1), the ratio of the magnetic and elastic contributions is determined by parameter $\beta = \mu_0 M_s^2/c_1$.

Analysis of function (1) shows that on the increase of the field the system passes a threshold above which two different equilibrium configurations of the particles exist simultaneously. One state is "remote", where the interparticle distance is slightly reduced in comparison with its initial value ($l \simeq l_0$). Another possible equilibrium is a "collapsed" one, where the particles converge to one another ($l \simeq 2a$). This bistabilty regime exists within a finite field-strength interval and ends up on further enhancement of the field, where only the collapsed state is stable. The consequence of this bistability is a hysteresis of the interparticle distance if the applied magnetic field change in cycle, see figure 2. In the systems where particle magnetization saturates, the possibility of hysteresis for a given initial distance between the particles $q_0 = l_0/a$ is controlled by parameter β that has the meaning of effective compliance of the system. For the reference magnetic characteristics of a real MRE and elasticity of the matrix $c_1 = 1.1$ kPa, parameter β of our model is about 2500.

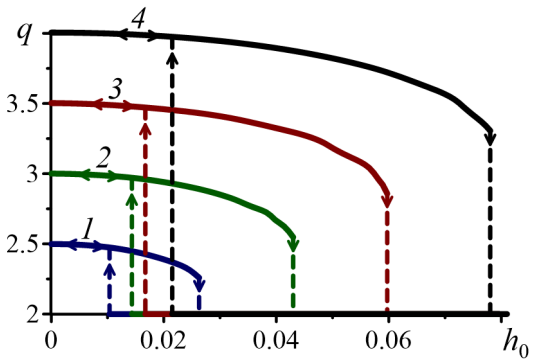

Figure 2. Magnetomechanical hysteresis for the mesoscopic element with $\beta = 2500$ and initial center-to-center distances q_0 equal 2.5 *(1)*, 3 *(2)*, 3.5 *(3)*, 4 *(4)*.

3. Elastic properties of the mesoscopic element

In the presence of external magnetic field h_0, the interparticle distance in the 2P element changes from the initial value l_0 to the new equilibrium one l. Simultaneously, the total length of the element decreases from L_0 to L. To account for that, we introduce the interparticle $\varepsilon_p = 1 - l/l_0$ and total $\varepsilon = 1 - L/L_0$ strains, and denote the equilibrium state of the element at h_0 as $(\varepsilon_p, \varepsilon)$.

An applied small (probing) force f causes an additional small deformation u of the element. Then the internal magnetic and elastic forces must change in order to balance this extra load, i.e., the sum of the sample energy and the work of the applied force must assume minimum:

$$U(\varepsilon_p, \varepsilon) - fu = \min . \tag{2}$$

This problem can be solved by expanding the energy in the vicinity of the equilibrium at $f = 0$. From that solution one obtains the parameter $K = f/\varepsilon$, that we term *effective rigidity*, characterizing the ability of the considered model to resist deformation:

$$\frac{f}{\varepsilon} = \left(A_{22} - \frac{A_{12}^2}{A_{11}} \right) \frac{1}{L_0}; \tag{3}$$

here A_{ij} are the second partial derivatives of the energy. Then the ratio $\tilde{K} = K(h_0)/K_0$, where $K(h_0)$ is the rigidity of the mesoscopic sample under a magnetic field and K_0 that calculated in its absence renders the field effect on the sample rigidity.

Since the interparticle distance in the element undergoes hysteresis, the rigidity should behave similarly. This conclusion is illustrated by figures 2 and 3, where, respectively, the field strength dependencies of the interparticle distances q and the reduced rigidity $\tilde{K}$ are presented.

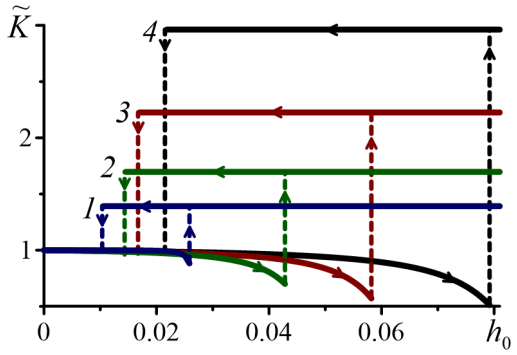

Figure 3. Rigidity of 2P mesoscopic elements with $\beta = 2500$ as a function of applied magnetic field; the initial interparticle distances q_0 are: 2.5 *(1)*, 3 *(2)*, 3.5 *(3)*, 4 *(4)* .

As figures 2 and 3 show, under the increase of the external field, first, the particles approach each other gradually that very slightly affects the rigidity of the system. Above a certain field strength (it depends on the interparticle distance), a second equilibrium configuration for the particle pair emerges, and this entails the second possible value of rigidity. As it is inherent to hysteretic systems, the actual rigidity of the system depends on the strain history. With further growth of the field, the bistability regime ends up, the collapsed state of the particles remains the only possible and, accordingly, the mesoscopic element acquires the enhanced rigidity.

4. Mesoscopic element under the action of external forces

The stress-strain dependence is a fundamental mechanical property of a material. To get a notion of how the external field affects this characteristic of our 2P structure element, let us consider a system with interparticle distance $q_0 = 3.25$ and a relative compliance $\beta = 2500$. Let a uniform magnetic field of strength $h_0 = 0.015$ be applied to the element along its axis. The set of parameters is chosen in such a way that in the force-free state the sample is in the bistability regime. Then on the end walls of the element a force of magnitude f, i.e., either compressing

(negative) or stretching (positive), is exerted. Using our model, we obtain the stress-strain diagram shown in figure 4a; here the dimensionless stress is defined as $p/c_1 = f/(c_1 S)$, where S is the cross section of the cylinder and c_1 the Mooney-Rivlin constant. Two possible rigidities of the system reflecting the mechanical responses of two different configurations of particles within the element cause the "doubling" of the diagram curves. In particular, they have different slopes in the absence of any mechanical load (see points *1* and *3*). An important circumstance revealed

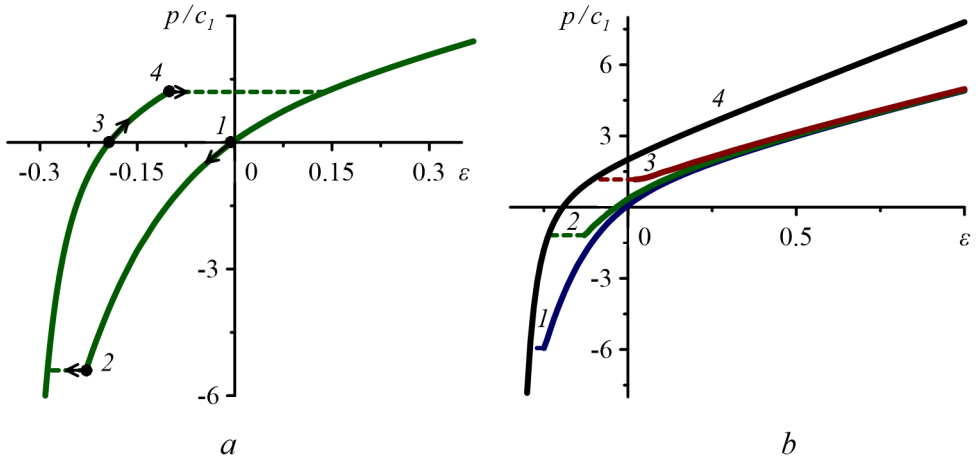

Figure 4. a) The stress-strain diagram for the mesoscopic element with compliance $\beta = 2500$ and initial interparticle distance $q_0 = 3.25$ under applied field $h_0 = 0.015$. b) The stress-strain diagram for the same mesoscopic element under variation of the applied field: $h_0 = 0.02$ *(1)*, 0.04 *(2)*, 0.06 *(3)*, 0.08 *(4)*; note that the latter diagram does not have a loop in the considered range of deformation and coincides with the upper curve of the other diagrams.

by figure 4 is that the increase of rigidity (caused by the particle collapse) can be provoked by an external mechanical load. If the 2P element is magnetized, it is already slightly shrunk even in the absence of an external mechanical force (see point *1*). This "load-free" compression is due to the well known *magnetostriction* effect inherent to MREs. A compressive force f causes further reduction of the element length, and at weak f the shrinking is gradual. However, when the force reaches a certain finite value, the particles collapse, and the strain changes abruptly (see point *2*). In terms of diagram 4a this means that the representing point jumps from the lower branch of the curve to the upper one and after that moves along the latter. It is noteworthy that, when the load is removed, the system does not return to its initial position (see point *3*) but remains in a compressed state, thus justifying the concept of a "magnetic staple" [12]. Indeed, one needs some effort in the opposite direction, a tensile force (see point *4*), to destroy this structure. Because of that, the graphic image of the loading / unloading cycle in figure 4 has a loop shape, whose boundaries projected on the vertical axis mark the boundaries of the bistability interval in terms of stress.

The above-presented considerations show that as soon as the mesoscopic element is prone to magnetomechanical hysteresis, then its stress-strain curve would be loop-shaped under the magnetic field of any intensity. This is illustrated in figure 4b that presents deformation cycles for the same mesoscopic element with $q_0 = 3.25$ and $\beta = 2500$. Note that a "magnetic staple" that has formed inside an element with high compliance is hard to destroy. For that, the sample should be stretched several times. Thus, in the diagram 4b for the element in the field 0.02 (cf. the diagram 4a) there is no reverse transition, see point *4*. In other words, as soon as "the magnetic staple" has once formed, it can break only under a substantial reduction or switching off of the field. The figure shows also that the position of the loop depends on the magnitude

of the applied field. Therefore, one sees that the mechanical properties of the 2P mesoscopic element could be field-tuned, thus increasing or reducing its ability to resist deformation.

5. Homogenization

The above-presented 2P model allows one to understand the basics of the MRE internal structure rearrangement and the subsequent change in the properties of those composites on the qualitative level. In order to predict the properties of macroscopic samples, it is necessary to subject our discrete model to some "homogenization". Several approaches of that kind were developed recently [13, 14, 15]. However, as our model takes into account only a single geometry—axially symmetrical layout of the particles with respect to the external magnetic field—in here we restrict our consideration by a very simple averaging procedure.

We present a macroscopic MRE sample to be an assembly of cylindrical samples—our 2P mesoscopic elements—whose initial interparticle distances q_0 are distributed according to a certain law. All the cylinder axes are pointing the same direction along which the external load is applied. Each element responds to it independently, as if it was cut from the whole sample. Thus, any interaction at the boundaries between the individual elements is neglected. Under these conditions, to calculate the elasticity modulus or the stretching / compression stress, one just needs to average the corresponding mesoscopic characteristics over q_0. This way of material modelling is known as the Voigt hypothesis.

As is easy to understand, the resulting continuum model of a MRE has as its prototype a set of 2P mesoscopic elements connected in parallel. Assuming that the number of structure elements in a macroscopic sample is very large, the averaging is done with a continuous distribution of the interparticle distances. Thus, the "homogenized" rigidity of the model MRE is defined as

$$\langle K(H_0)\rangle = \left[\int_0^{q_0^{max}} K(q_0, h_0)\, f(q_0)\, dq_0\right] \Big/ \left[\int_0^{q_0^{max}} F(q_0)\, dq_0\right], \tag{4}$$

where function $F(q_0)$ renders distribution of the pairs with respect to q_0. As an example, we assume quasi-normal distribution of the distances. That means that when discretizing the standard formula for $F(q_0)$ we, first, limit ourselves by only non-negative values of q_0 and, second, truncate the distribution at $q_0 = 4.25$ since this is the largest center-to-center distance that our calculational scheme of the 2P element allows us to deal with. These restrictions are taken into account in order to have $F(q_0)$ normalized to unity. Keeping the form of the function, we set in it the "mean value" $\langle q_0\rangle = 3.0$ and "standard deviation" $\sigma = 0.3$. The resulting curve is shown in figure 5. As seen, with the field growth the rigidity of the model macroscopic sample, first, slightly decreases, and then increases. The rate of increase slows down gradually and finally tends to zero when saturation regime is attained. The second part of the cycle (field diminution) reveals the hysteresis loop of $\tilde{K}(h_0)$ of a considerable width.

The behavior of $\tilde{K}(h_0)$ can be easily explained with the help of figure 3 that renders the rigidity changes of 2P mesoscopic elements with different q_0's. When the field is turned on, the particles move towards each other and the stiffness decreases in all the elements. At the field strength about 0.02, two different rigidities become available, see figure 5. As the field is increased, the elements with smallest q_0's are first to collapse. However, the increase of rigidity induced by such pairs is not enough to counterbalance the decrease induced by the elements with larger q_0, where the particles are yet at the first stage of convergence. In the considered assembly, the majority of the pairs has the initial interparticle distances close $q_0 = 3$. Because of that, in the field $h_0 = 0.045$ that provokes the collapse of those pairs, the rigidity undergoes a fast increases. In the field $h_0 = 0.06$ even particles that were at the farthest initial distance are forced to collapse, and the sample rigidity saturates.

The stress–strain diagrams could be averaged similarly. In figure 6a the dashed line shows the diagram for the MRE sample loaded in the absence of a magnetic field. Solid lines show

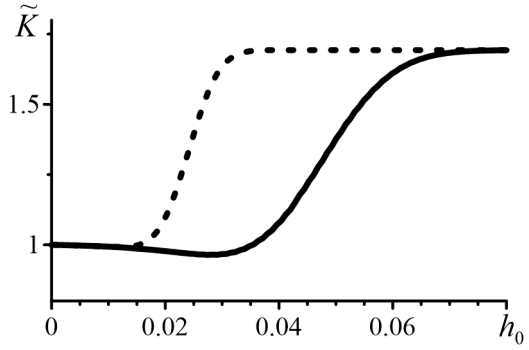

Figure 5. Relative rigidity of the model MRE sample corresponding to quasi-normal distribution of the 2P elements with $\langle q_0 \rangle = 3.0$ and $\sigma = 0.3$ as a function of external magnetic field.

the diagram obtained in the field $h_0 = 0.04$. The point marks the initial state of the sample in the field, that is, the equilibrium magnetically induced deformation under zero external stress. According to figure 5, the rigidity of this MRE in the field $h_0 = 0.04$ increases by about 10%, so the slopes of the lower curve of the diagram in the initial position and the dashed curve differ just a little.

So, one sees that, in general, the considered macroscopic MRE sample inherits the behavior of its mesoscopic elements, with exception that the transitions between the the lower and upper branches occurs smoothly. The conclusion that the stronger applied field the higher rigidity of the composite in the initial state is also confirmed by the stress-strain diagram 6b, where the slopes of the curves increase from point *1* to point *3* for successively increasing field strengths.

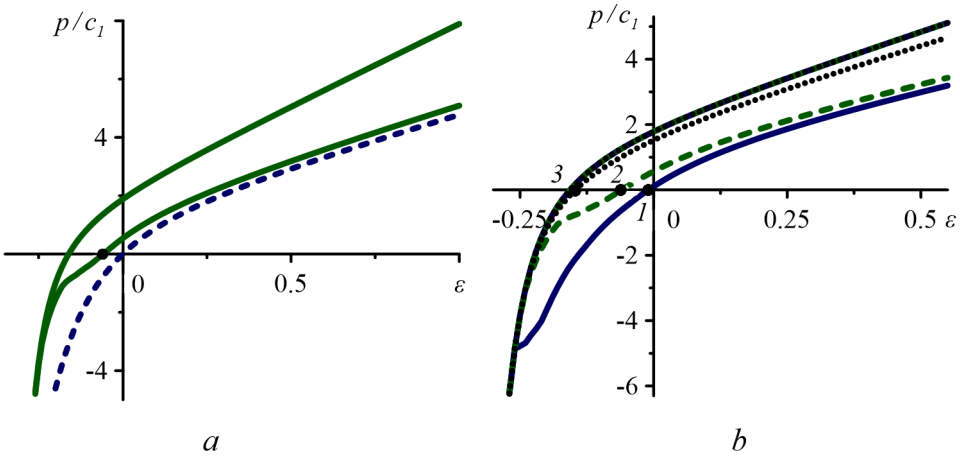

Figure 6. Stress-strain diagrams for the model MRE sample with relative compliance $\beta = 2500$: a) in the absence of magnetic field (dashes) and under the field $h_0 = 0.015$ (solid line); b) in the field $h_0 = 0.02$ (solid line), 0.04 (dashes), 0.06 (dots). The points mark the respective field-induced deformations under zero external stress.

6. Conclusions

The model of a 2P mesoscopic structure element developed in Refs. [7, 8] was specialized to describe the inner deformations which occur in MREs, which are free of external mechanical

stress, under the action of an applied magnetic field. Herein, this model is extended for the case where the element is subjected to a uniaxial load. This allows us to analyze the combined magnetomechanical effects in the mesoscopic model system.

In particular, we show that a pure mechanical load is able to produce a strain hysteresis in a 2P element that otherwise dwells in an equilibrium magnetized state. In a qualitative way this proves that clustering of the particles (occurrence of "magnetic staples"), which changes so much the macroscopic properties of the MREs, could be provoked by mechanical loads as well as by magnetization as such.

An attempt to bridge the built up mesoscopic description with the macroscopic evidence is done. In spite of a very simple approach (Voigt hypothesis), the predictions look reasonable, promising and helpful for interpretation of the experimental data.

Acknowledgments

This work was supported by the Basic Research Program of Ural Branch of RAS No.10 (15-10-1-18), RFBR project 16-31-00503 and RFBR-DFG project 16-51-12001 (PAK 907).

References

[1] Zrínyi M, Barsi L and Büki A 1996 *Journal of Chemical Physics* **104** 8750–8756
[2] Nikitin L V, Mironova L S, Stepanov G V and Samus A N 2001 *Polymer Science, series A* **43** 443–450
[3] Ginder J M, Clark S M Schlotter W F and Nichols M E 2002 *International Journal of Modern Physics B* **16** 2412–2418
[4] Stolbov O V, Raikher Yu L and Balasoiu M 2011 *Soft Matter* **7** 8484–8487
[5] Ivaneyko D, Toshchevikov V P, Saphiannikova M and Heinrich G 2012 *Condensed Matter Physics* **15** 411–424
[6] Han Y, Hong W and Faidley L E 2013 *International Journal of Solids and Structures* **50** 2281–2288
[7] Biller A M, Stolbov O V and Raikher Yu L 2014 *Journal of Applied Physics* **116** 114904
[8] Biller A M, Stolbov O V and Raikher Yu L 2015 *Physical Review E* **92** 023202
[9] Bozorth R M 1993 *Ferromagnetism* (Wiley-IEEE Press)
[10] Oswald P 2009 *Rheophysics: The Deformation and Flow of Matter* (Cambridge University Press)
[11] Stepanov G V, Abramchuk S S, Grishin D A, Nikitin L V, Kramarenko E Yu and Khokhlov A R 2007 *Polymer* **48** 488–495
[12] Melenev P V, Rusakov V V and Raikher Yu L 2006 *Journal of Magnetism and Magnetic Materials* **300** e187–e190
[13] Ponte Castañeda P and Galipeau E 2011 *Journal of Mechanics and Physics of Solids* **59** 194–215
[14] Menzel A 2014 *Journal of Chemical Physics* **141** 194907
[15] Romeis D, Toshchevikov V and Saphiannikova M 2016 *Soft Matter* **12** 9364–9376